J. Fluid Mech. (1981), *vol.* 104, *pp.* 505–526
Printed in Great Britain

Head-sea diffraction by a slender raft with application to wave-power absorption

By PIERRE HAREN AND CHIANG C. MEI

Parsons Laboratory, Department of Civil Engineering,
Massachusetts Institute of Technology, Cambridge, Mass. 02139

(Received 22 April 1980 and in revised form 1 August 1980)

The parabolic approximation which has recently been found to be useful in other physical contexts, is extended to head-sea diffraction of short waves by a slender raft on deep water. In particular, it is a much more direct way of getting the inner approximation of the outer solution in a scheme of matched asymptotics than the original method of Faltinsen (1971). The present results are compared with a more involved integral equation method and are found to be remarkably accurate even when the raft length is comparable to the wavelength. Finally, the asymptotic method is modified for a compliant raft which absorbs wave power by suitably controlled impedance. Optimum efficiency and other performance characteristics are predicted.

1. Introduction

The scattering problem of a slender body in head seas has received considerable attention since Ursell (1968) proved that the velocity potential of a head-sea propagating along an infinitely long horizontal cylinder must increase linearly with the transverse distance, thus becoming unbounded at infinity. Using Ursell's solution as the inner approximation in a scheme of matched asymptotics, Faltinsen (1971) solved the head-sea diffraction of short waves by a slender body of circular cross-section; the solution is, however, singular at the bow. For the same problem, Maruo & Sasaki (1974) derived an improved solution which was finite everywhere and compared well with experimental results. Further progress is being made by Skjørdal & Faltinsen (1980) and Liapis & Faltinsen (1980) for slender bodies of arbitrary cross-section. The accuracy of this asymptotic method has so far not been compared with other more exact methods. In all these works the far-field solution was first formulated as a distribution of sources and dipoles on the longitudinal axis of the body. The inner expansion of this far field must be deduced after considerable manipulation before matching with the outer expansion of the near-field solution and leading to an Abel integral equation. Recent work by Mei (1979) for elastic waves on slender cracks and Mei & Tuck (1980) for shallow water waves on slender islands show that the parabolic approximation avoids the intricate mathematics needed to seek an inner expansion of the outer solution by singularity distributions and leads rapidly to similar Abel's integral equations. One of the principal aims of this paper is to extend the use of parabolic approximation to water waves. For our own practical goals only the case of a slender raft of zero draft is demonstrated, but modifications for arbitrary cross-section are straightforward. The second aim is to assess the accuracy of the asymptotic

0022-1120/81/4661-3500 $02.00

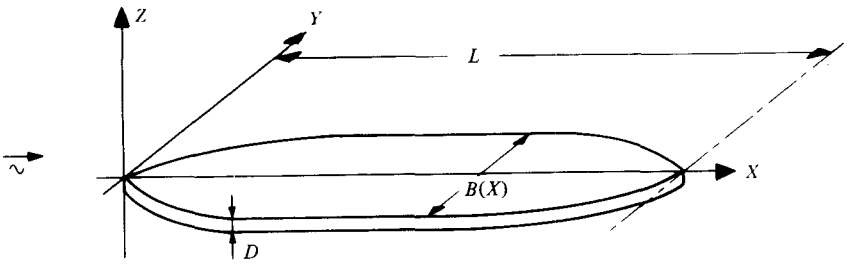

FIGURE 1. Notation.

method by comparing with a direct integral equation method which is much more cumbersome, though not restricted to slender bodies or head seas. The asymptotic method is then further modified for studying the characteristics of a wave-power device.

2. Formulation of the scattering problem

Consider head-sea incidence on an elongated body in deep water (see figure 1). The body is assumed to be symmetric with respect to its longitudinal axis, which is in the direction of the incident wave. The exact linearized boundary-value problem for the diffraction potential $\Phi(X, Y, Z, T)$ is governed by the following conditions:

$$\Delta\Phi = 0 \quad \text{for} \quad Z < 0; \tag{2.1}$$

$$\Phi_n = 0 \quad \text{on the body } B; \tag{2.2}$$

$$\omega^2\Phi/g - \Phi_Z = 0 \quad \text{on the free surface } F(Z = 0); \tag{2.3}$$

$$\Phi \to 0 \quad \text{as} \quad Z \to -\infty; \tag{2.4}$$

$$(\Phi - \Phi^I) \to \exp\left(i(KR - \omega T) + KZ\right)\left(-\frac{iA(\theta)g}{\omega(KR)^{\frac{1}{2}}}\right) \quad \text{as} \quad KR = K(X^2 + Y^2)^{\frac{1}{2}} \to \infty, \tag{2.5}$$

where Φ^I is the incident wave potential

$$\Phi^I = -Aig\exp\left[KZ + i(KX - \omega T)\right]/\omega \quad \text{with} \quad K = \omega^2/g. \tag{2.6}$$

From here on, we normalize all lengths by the body length L and define the normalized potential ϕ in the following way:

$$\Phi(X, Y, Z, T) = -\frac{igA}{\omega}\phi(x, y, z)\, e^{-i\omega T}, \tag{2.7}$$

where A is the incident wave amplitude.

As our own practical goal in this study is for scattering by a floating raft with draft D very much less than the beam B, we assume further that

$$D/B \ll 1. \tag{2.8}$$

All numerical results to be presented are subject to (2.8). However, it is not difficult to extend the present work to arbitrary cross-sectional shape.

With (2.8) the dimensionless boundary-value problem becomes

$$\Delta\phi = 0 \quad \text{in} \quad z < 0, \tag{2.9}$$

$$k\phi - \phi_z = 0 \quad \text{on} \quad z = 0 \quad (\text{domain } F), \tag{2.10}$$

$$\phi_z = 0 \quad \text{on} \quad z = 0 \quad (\text{domain } R), \tag{2.11}$$

$$\phi \to 0 \quad \text{as} \quad z \to -\infty, \tag{2.12}$$

$$\phi - \phi^I \to a(\theta) r^{-\frac{1}{2}} e^{ikr+kz} \quad \text{as} \quad kr = (x^2+y^2)^{\frac{1}{2}} \to \infty \tag{2.13}$$

with

$$\phi^I(x,y,z) = e^{kz+ikx}. \tag{2.14}$$

Finally, we shall focus our attention on a slender body and short waves, so that

$$k = KL \gg 1 \quad \text{and} \quad b = B/L \ll 1 \quad \text{while} \quad kb = KB = O(1). \tag{2.15}$$

Because of these assumptions, it is natural to employ the method of matched asymptotic expansions.

3. The method of matched asymptotics via parabolic approximation

3.1. *The inner field potential*

Following Ursell (1968) and Faltinsen (1972), we factor out a rapidly varying part and write

$$\phi(x,y,z) = E(x,y,z)e^{ikx}. \tag{3.1}$$

From (2.9) we find

$$E_{yy} + E_{zz} - k^2E = -E_{xx} - 2ikE_x \quad \text{on} \quad z < 0. \tag{3.2}$$

However, near the body E_{zz} and E_{yy} are $O(b^{-2}E)$ while $E_x = O(E)$ because E is expected to vary slowly in x on the scale of the body length. Therefore, we neglect the last two terms in (3.2) and obtain, with a relative error of $O(b)$:

$$E_{yy} + E_{zz} - k^2E = 0, \quad z < 0, \quad y \leqslant O(b), \tag{3.3}$$

$$kE - E_z = 0, \quad z = 0 \quad (\text{domain } F); \tag{3.4}$$

$$E_z = 0, \quad z = 0 \quad (\text{domain } R); \tag{3.5}$$

$$E \to 0, \quad z \to -\infty. \tag{3.6}$$

Lastly, the boundary condition for large $k|y|$ must be dictated by matching the outer expansion of this inner field potential to the inner expansion of the outer field potential. For this matching to be possible, we must require the inner field potential not to grow exponentially in $k|y|$. This condition was first used by Ursell (1968). As was pointed out by Faltinsen, the inner problem is formally Ursell's problem for an infinitely long cylinder.

We shall now solve the inner problem with a Green function and an integral equation. It is convenient to decompose E as follows,

$$E(x,y,z) = F''(x)\,(e^{kz} + F'(x,y,z)), \tag{3.7}$$

where F' and F'' are unknown. The part F' is clearly governed by (3.3), (3.4), (3.6) and

$$F'_z = -k, \quad z = 0, \quad -b(x) \leqslant y \leqslant b(x); \tag{3.8}$$

$$F' \text{ does not grow exponentially as } k|y| \to \infty. \tag{3.9}$$

The function $F''(x)$ is to be found by matching with the outer solution. Let us observe that $F''(x)e^{kz}$ is a homogeneous solution of (3.3)–(3.6). Because both F' and F'' are so far unknown, there is no loss of generality to require that F' does not contain any homogeneous solution.

Let us define the Green function $g(y, z; y_0)$ by the following set of conditions:

$$g_{yy} + g_{zz} - k^2 g = 0 \quad \text{in} \quad z < 0; \tag{3.10}$$

$$kg - g_z = \delta(y - y_0) \quad \text{on} \quad z = 0; \tag{3.11}$$

$$g \to 0 \quad \text{as} \quad z \to -\infty; \tag{3.12}$$

$$g \text{ has no free wave } e^{kz} \text{ and does not grow exponentially in } k|y|. \tag{3.13}$$

It is easy to see that a formal representation for F' is

$$F'(x, y, z) = \int_{-\frac{1}{2}b(x)}^{\frac{1}{2}b(x)} (kF'(x, y_0, 0) - F'_z(x, y_0, 0)) g(y, z; y^0) dy_0, \tag{3.14}$$

which satisfies (3.3), (3.4), (3.6) and (3.9). Invoking the remaining boundary condition (3.8) on the raft, we get the following Fredholm integral equation of the second kind for F':

$$F'(x, y, 0) = \int_{-\frac{1}{2}b(x)}^{\frac{1}{2}b(x)} g(y, 0; y_0) [kF'(x, y_0, 0) + k] dy_0. \tag{3.15}$$

Notice that F' is only parametrically dependent on x through $b(x)$. We shall write

$$F'(y) = F'(x, y, 0) \tag{3.16}$$

and $y = u/k$ to obtain the final transverse integral equation,

$$F'(u/k) = \int_{-\frac{1}{2}kb(x)}^{\frac{1}{2}kb(x)} g(u/k, 0; u_0/k) (F'(u_0/k) + 1) du_0. \tag{3.17}$$

The full expression for $g(y, z; y_0)$ is derived in appendix,

$$g(y, z; y_0) = k|y - y_0| e^{kz} - \frac{1}{\pi} \int_k^\infty \frac{\exp(-v|y - y_0|)}{v^2} [k \sin(z(v^2 - k^2)^{\frac{1}{2}}) + (v^2 - k^2)^{\frac{1}{2}} \cos(z(v^2 - k^2)^{\frac{1}{2}}] dv, \tag{3.18}$$

from which we get the kernel for (3.17)

$$g(y, 0; y_0) = k|y - y_0| - \frac{1}{\pi} K_0(k|y - y_0|) + \frac{1}{\pi} \int_0^\infty \frac{\exp(-k|y - y_0| \cosh u)}{\cosh^2 u} du. \tag{3.19}$$†

† Garrison (1969) studied obliquely incident waves on an infinitely long raft of constant width. While (3.2)–(3.6) still apply with k replaced by $k \sin \beta$ (β = incident angle, $\frac{1}{2}\pi$ for head seas), his radiation condition that scattered waves are outgoing as $|ky| \to \infty$ does not show linear growth in the limit of head seas ($\beta \to \frac{1}{2}\pi$). In particular Garrison's Green's function (equation (32)) does not reduce to our (3.19).

Now (3.17) may be solved numerically for each x. Once $F'(y)$ is known, the inner potential is given formally by

$$\phi(x,y,z) = e^{ikx}F''(x)\left[e^{kz} + k\int_{-\frac{1}{2}b(x)}^{\frac{1}{2}b(x)} (1+F'(y_0))\,g(y,z;y_0)\,dy_0\right]. \tag{3.20}$$

For matching with the outer solution we need the asymptotic expansion of ϕ for large $k|y|$. It is shown in appendix that

$$g(y,z;y_0) = k|y-y_0|\,e^{kz} + O(\exp[-k|y-y_0|]), \quad k|y-y_0| \gg 1. \tag{3.21}$$

Upon substituting (3.21) in (3.20) we find

$$\phi(x,y,z) \sim e^{ikx+kz}F''(x)\left[1 + k^2|y|\int_{-\frac{1}{2}b(x)}^{\frac{1}{2}b(x)} (1+F'(y_0))\,dy_0\right], \quad k|y-b| \gg 1. \tag{3.22}$$

Equation (3.22) gives the outer expansion of the inner approximation. We now turn our attention to the outer potential.

3.2. *The outer potential and the parabolic approximation*

In view of the slender body assumption and the outer approximation of the inner solution (3.22), we assume for the outer potential

$$\phi(x,y,z) = F(x,y)e^{ikx+kz} \quad \text{for} \quad k|y| \gg 1. \tag{3.23}$$

Equation (2.9) now reads

$$F_{xx} + F_{yy} + 2ikF_x = 0. \tag{3.24}$$

For large k, $F_{xx}/2ikF_x = O(k^{-1}) \ll 1$. The region where F_{yy} and $2ikF_x$ are of the same order of magnitude must be such that $y = O(k^{-\frac{1}{2}})$. With F_{xx} neglected, the approximate equation is

$$F_{yy} + 2ikF_x = 0 \quad \text{in} \quad x = O(1), \quad y = O(k^{-\frac{1}{2}}), \tag{3.25}$$

which is referred to as the parabolic approximation. Clearly (3.25) is appropriate only in an intermediate field and not in the far field $k(x^2+y^2)^{\frac{1}{2}} \gg 1$, where radiation is the important feature. However, it is sufficient for solving the near field, which is often the region of practical interest.

For a slender body with $db(0)/dx \leqslant O(1)$, back-scattering is expected to be small and it is reasonable to assume that

$$F(x,y) = 1 \quad \text{for} \quad x \leqslant 0. \tag{3.26}$$

The radiation condition for $(\phi - \phi^I)$ is now replaced by the weaker condition

$$(\phi - \phi^I) \to 0 \quad \text{for} \quad k|y| \to \infty$$

or

$$F(x,y) \to 1 \quad \text{for} \quad k|y| \to \infty. \tag{3.27}$$

To the outer observer in $y = O(k^{-\frac{1}{2}})$, the body appears to be lying on $y = 0$ and the following flux condition may be formally imposed,

$$\partial F/\partial y = \pm V(x) \quad \text{at} \quad y = 0\pm. \tag{3.28}$$

Symmetry with respect to the y axis has been used. $V(x)$ is to be found by matching with the inner problem. The outer problem resembles the conduction of heat in a semi-infinite rod and may be readily solved, as in Mei & Tuck (1980),

$$F(x,y) = 1 - \frac{1+i}{2(\pi k)^{\frac{1}{2}}} \int_0^x \frac{d\xi\, V(\xi)}{(x-\xi)^{\frac{1}{2}}} \exp\left[iky^2/2(x-\xi)\right]. \tag{3.29}$$

The inner approximation of the outer potential is, as $|y|$ goes to 0:

$$\phi(x,y,z) = e^{ikx+kz}(F_0(x) + |y|\, V(x) + O(y^2)), \tag{3.30}$$

where

$$F_0(x) = 1 - \frac{1+i}{2(\pi k)^{\frac{1}{2}}} \int_0^x \frac{d\xi\, V(\xi)}{(x-\xi)^{\frac{1}{2}}}. \tag{3.31}$$

3.3. *Matching and derivation of the longitudinal integral equation*

Requiring that expressions (3.30) and (3.22) should match in the overlapping region $k^{-1} \ll |y| \ll k^{-\frac{1}{2}}$, we obtain

$$1 - \frac{1+i}{2(\pi k)^{\frac{1}{2}}} \int_0^x \frac{d\xi\, V(\xi)}{(x-\xi)^{\frac{1}{2}}} = F''(x) \tag{3.32}$$

and, since the problem is symmetric with respect to the plane (x,z),

$$V(x) = F''(x)\, k^2 \left[b(x) + 2\int_0^{\frac{1}{2}b(x)} F'(y)\, dy\right]. \tag{3.33}$$

Elimination of $F''(x)$ gives the final integral equation for the longitudinal variation of V:

$$1 - \frac{1+i}{2(\pi k)^{\frac{1}{2}}} \int_0^x \frac{d\xi\, V(\xi)}{(x-\xi)^{\frac{1}{2}}} = \frac{V(x)}{k^2\left[b(x) + 2\int_0^{\frac{1}{2}b(x)} F'(y)\, dy\right]}. \tag{3.34}$$

Once $V(x)$ is found, equation (3.22) or (3.23) gives $F''(x)$ and the potential under the body is then given by

$$\phi(x,y,0) = e^{ikx} F''(x)\,[1 + F'(y)]. \tag{3.35}$$

In summary, we first solve for $F'(y)$ at each cross-section x by solving the transverse integral equation (3.17) and then solve the longitudinal Abel integral equation (3.34) for $V(x)$.

A quantity of interest is the integrated pressure over a lateral cross-section of the body, which gives the vertical force $\mathscr{F}(x)$ per unit length of the raft. It is easy to prove from (2.7), (3.33) and (3.35) that the dimensional force $\mathscr{F}(x)$ and its normalized counterpart $f(x)$ are given by

$$\mathscr{F}(x) = \rho g A L f(x) = \rho g A L\, e^{ikx}\, V(x) k^{-2}. \tag{3.36}$$

In the special case of constant cross-section, $b(x) = b$ on $0 \leqslant x \leqslant 1$, the solution of (3.34) can be obtained explicitly as in Mei & Tuck (1980), yielding

$$V(x) = \frac{\exp(ix/2k\sigma^2)}{\sigma} \operatorname{erfc}\left(\frac{(1+i)x^{\frac{1}{2}}}{2k^{\frac{1}{2}}\sigma}\right) \tag{3.37}$$

with

$$\sigma^{-1} = k^2\left(b + 2\int_0^{\frac{1}{2}b} F'(y)\, dy\right). \tag{3.38}$$

This solution is expected to give accurate results only when kb is sufficiently small. For large kb some reflexion is expected at the bow and (3.26) is no longer valid. Quantitative checks will be discussed later. Lastly, it is worth noticing that, with (3.37), the asymptotic expansion of (3.35) leads to

$$\phi(x,y,0) \to \frac{e^{ikx}}{k}\left(\frac{2}{\pi}\right)^{\frac{1}{2}} \frac{e^{-\frac{1}{4}i\pi}}{(kx)^{\frac{1}{2}}} \frac{1+F'(y)}{\left(b+2\int_0^{\frac{1}{2}b} F'(y)dy\right)} \quad \text{as} \quad kb(kx)^{\frac{1}{2}} \to \infty, \tag{3.39}$$

which is consistent with Faltinsen's (1971, 1972) and Ursell's (1977) results for a long circular cylinder, but much more easily derived.

Finally, we remark that, for arbitrary cross-sections, the only modification needed is in the inner solution. For example, for a body symmetrical about the vertical plane (x,z), Ursell's source distribution method may be used. The source strength $\mu(s)$ along the body contour is determined from a Fredholm integral equation similar to (2.15). Ursell has also shown that the outer expansion of the potential is

$$\phi(x,y,z) \to e^{ikx}\, e^{kz}\left(1 + k^2|y|\, 4\pi \int_{C_+} \mu(s)\, e^{kz(s)} ds\right), \quad k|y| \to \infty, \tag{3.40}$$

where C_+ is the body contour on the side $y > 0$. The remaining task of matching with the outer solution proceeds just as before. Liapis & Faltinsen (1980) recently improved the numerical efficiency of the solution of the inner problem for arbitrary cross-section by replacing the distribution of complicated Green's functions over the body section by a distribution of simple Green's functions over the body section and the free surface. For finite depth it is also straightforward to modify the hybrid element method of Chen & Mei (1974), Bai & Yeung (1974) and Yue, Chen & Mei (1978) for conventional diffraction problems.

For the sake of evaluating the asymptotic method, an integral equation method will also be used, as sketched below.

4. Integral equation method

For the sake of verifying the asymptotic method, we apply a more numerical method which solves the exact boundary-value problem for a zero draft body. The integral equation involved is essentially due to W. D. Kim (1963) who studied an elliptical disk. However a more general solution scheme using triangular elements is used here as in Yeung (1973) in another context. The linearized boundary-value problem for the scattering potential Φ^S, where $\Phi = \Phi^I + \Phi^S$, is governed by (2.1), (2.3), (2.4), (2.5) and

$$\Phi^S_Z = -\Phi^I_Z \quad \text{on the body (domain } B). \tag{4.1}$$

The pressure amplitude under the body is given by

$$P(X) = \frac{ip\rho g}{\omega}\left[\frac{\omega^2}{g}(\Phi^S + \Phi^I)\right] = \frac{i\rho g}{\omega}\left(\frac{\omega^2\Phi^S}{g} + \Phi^I_Z\right). \tag{4.2}$$

To obtain Φ^S we use a Green function $G(\mathbf{x}, \mathbf{x}_0)$ which corresponds to the potential due

to a point pressure externally applied on the free surface (without free waves) and satisfies (2.1), (2.4), and (2.5) together with

$$\frac{i\rho g}{\omega}\left(\frac{\omega^2 G}{g} - G_Z\right) = \delta(X - X_0)\,\delta(Y - Y_0) \quad \text{on} \quad Z = 0. \tag{4.3}$$

In terms of G, Φ^S can be written formally as

$$\Phi^S(X, Y, Z) = \iint_B \frac{i\rho g}{\omega}\left[\frac{\omega^2}{g}\Phi^S(X_0, Y_0, 0) - \Phi^S_Z(X_0, Y_0, 0)\right] \times G(X, Y, Z; X_0, Y_0, 0)\,dX_0 dY_0. \tag{4.4}$$

Incorporating the boundary condition (4.1) in (4.4), we obtain the final integral equation

$$\Phi^S(X, Y, 0) = \iint_B \frac{i\rho g}{\omega}\left[\frac{\omega^2}{g}\Phi^S(X_0, Y_0, 0) + \Phi^I_Z(X_0, Y_0, 0)\right] \times G(X, Y, Z; X_0, Y_0, 0)\,dX_0\,dY_0. \tag{4.5}$$

It is now natural to normalize all length scales involved by $K = \omega^2/g$ and we thus define the following dimensionless variables:

$$\mathbf{x} = \omega^2/g\mathbf{X}, \tag{4.6}$$

$$\Phi^S = \frac{-igA}{\omega}\phi(\mathbf{x})\,e^{-i\omega T}, \tag{4.7}$$

$$g(\mathbf{x}, \mathbf{x}_0) = \frac{i\rho g^2}{\omega^3} G(\mathbf{X}, \mathbf{X}_0). \tag{4.8}$$

The dimensionless integral equation is

$$\phi(x, y, 0) = \iint_B (\phi + e^{ix})(x_0, y_0, 0)\, g(x, y, 0; x_0, y_0, 0)\,dx_0\,dy_0. \tag{4.9}$$

The solution for g can be found by Fourier transform (Haren 1980)

$$g(x, y, z; x_0, y_0, 0) = -\frac{1}{2\pi r} + \frac{e^z}{4}[\mathbf{H}_0(\rho) + Y_0(\rho) - 2i\,J_0(\rho)] + \frac{e^z}{2}\int_z^0 \frac{e^{-t}\,dt}{(t^2+\rho^2)^{\frac{1}{2}}}. \tag{4.10}$$

where $\mathbf{H}_0$ denotes Struve function and

$$\rho = ((x - x_0)^2 + (y - y_0)^2)^{\frac{1}{2}}, \quad r = (\rho^2 + z^2)^{\frac{1}{2}}. \tag{4.11), (4.12}$$

Eq. (4.10) is in principle a limit of the submerged source potential derived by Haskind (1954) and quoted in Wehausen & Laitone (1960, p. 477), when the submergence becomes zero. Now the form of this Green's function is very much simpler than that commonly used in existing numerical integral equation methods. For $z = 0$ it further reduces to the same Green's function used by Kim (1963):

$$g(x, y, 0; x_0, y_0, 0) = -\frac{1}{2\pi\rho} + \tfrac{1}{4}[\mathbf{H}_0(\rho) + Y_0(\rho) - 2i\,J_0(\rho)]. \tag{4.13}$$

With (4.13), (4.9) can be solved numerically. For a body symmetrical about the x axis, we partition the half $y \geqslant 0$ into triangles over each of which the potential ϕ is assumed to vary linearly. The unknowns are the values of ϕ at the nodes and a linear system of

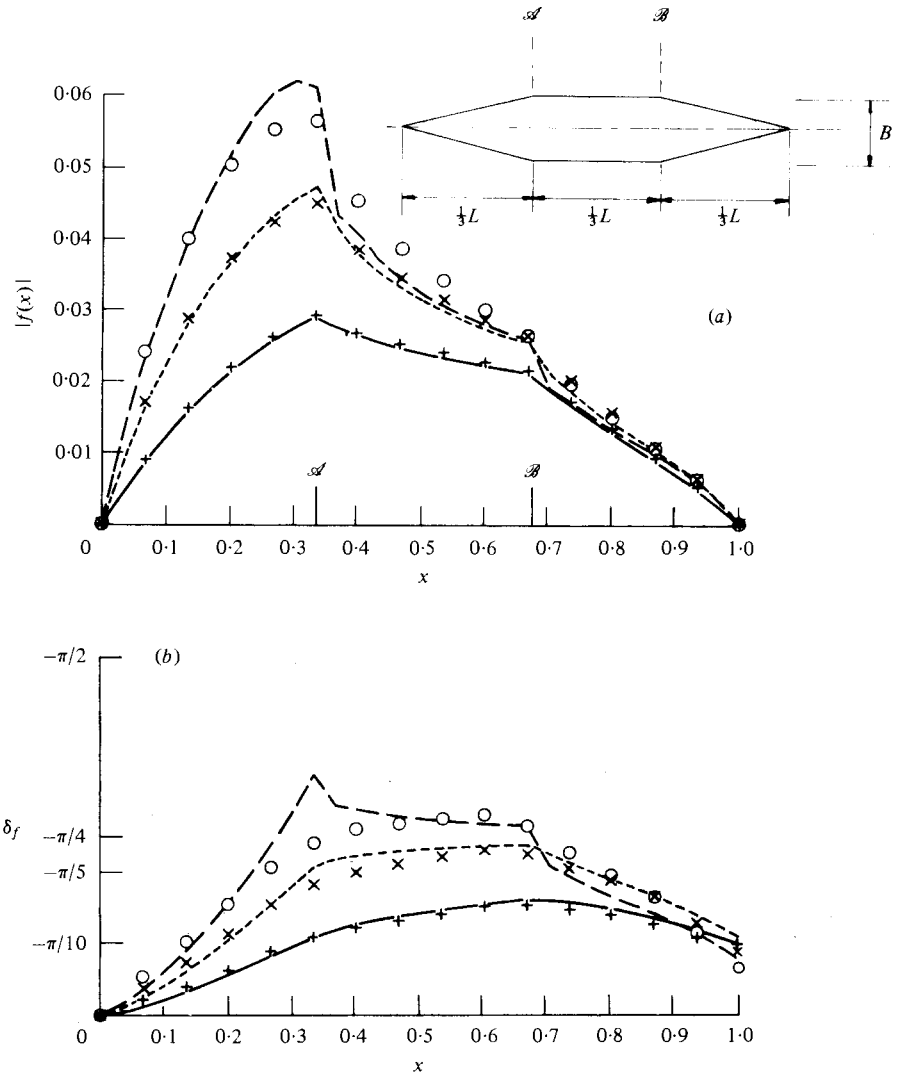

FIGURE 2. Normalized force $f(x)$ along rafts of P class with $L/\Lambda = 2$. For $B/L = 0{\cdot}005$, $0{\cdot}1$, $0{\cdot}15$ respectively: ——, – – – –, — —, asymptotic theory; ○, ×, +, integral equation. (*a*) Amplitude $|f|$; (*b*) phase of $fe^{-ikx} = \delta_f$.

algebraic equations is obtained by applying (4.9) at all of the nodes. The complex matrix equation is inverted by a standard routine. A detailed description of all the numerical computations can be found in Haren (1980). All the results presented are renormalized as in §2 for comparison with the asymptotic theory.

5. Comparison of two methods

We first examine two families of rafts with triangular ends of length $\frac{1}{3}L$ joining a rectangular centre piece. Family P corresponds to $k = 4\pi$ while family Q corresponds to $k = 2\pi$. Within each family there are three rafts, to be labelled by P_i or Q_i with

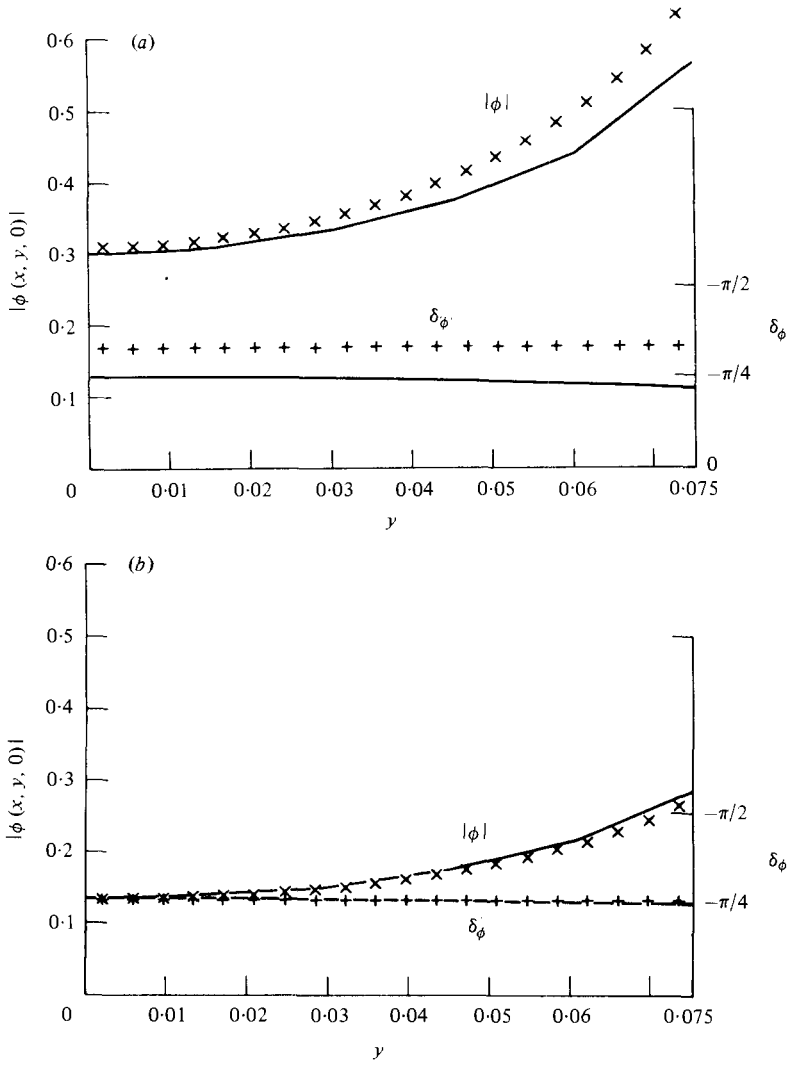

FIGURE 3. Normalized potential across the raft P_3 with $L/\Lambda = 2$ and $B/L = 0{\cdot}15$. ×, +, asymptotic theory; ——, integral equation, where δ_ϕ = phase of ϕe^{-ikx}. (*a*) Section $\mathscr{A}$ at $x = \frac{1}{3}$; (*b*) section $\mathscr{B}$ at $x = \frac{2}{3}$.

$i = 1, 2, 3$ corresponding to increasing slenderness ratio $B/L = 0{\cdot}05$, $0{\cdot}1$ and $0{\cdot}15$ respectively.

For family P where $L = 2\Lambda$, Λ being the wavelength, the value of k is not very large. The vertical force $f(x)$ along the raft is shown in figure 2(*a*) for the magnitude and figure 2(*b*) for the phase. The agreement of the two methods is very good for P_1 and P_2. For the widest raft P_3 ($kb = 1{\cdot}885$) discrepancies begin to be appreciable along the raft near the sharp corners. For the raft P_3 (the worst case) we also compared in figures 3(*a*) and 3(*b*) the beamwise variation of $\phi(x, y)$ at two fixed sections $\mathscr{A}$ and $\mathscr{B}$, which correspond to the fore and aft ends of the rectangular piece. Some discrepancies exist in both magnitude and phase along the forward section $\mathscr{A}$ while the agreement is vastly improved at the backward section $\mathscr{B}$.

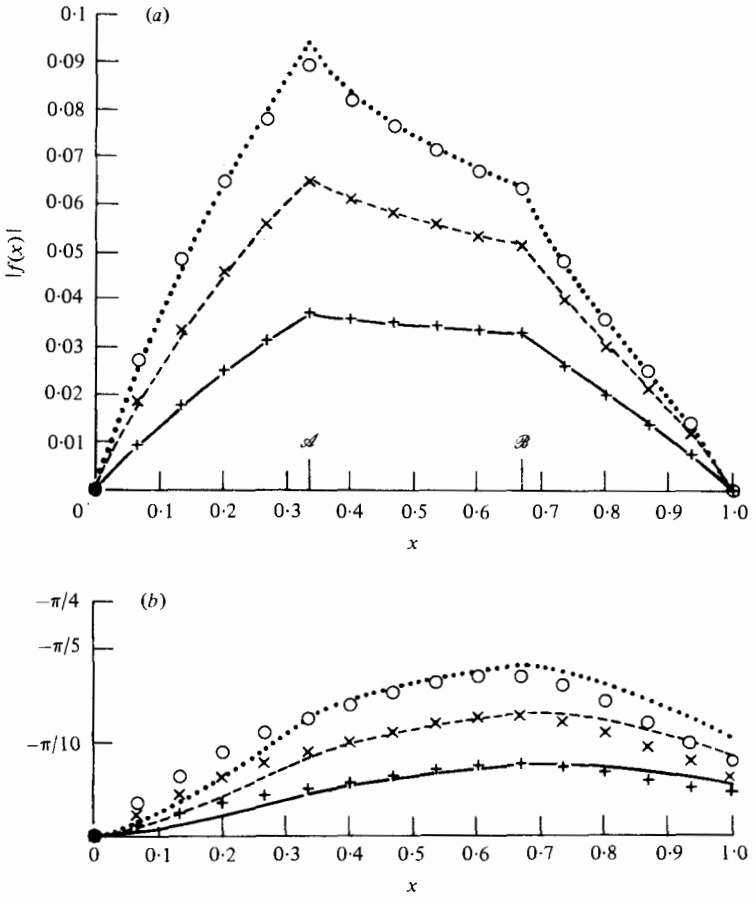

FIGURE 4. Normalized force along rafts of Q class with $L/\Lambda = 1$. For $B/L = 0{\cdot}05$, $0{\cdot}1$, $0{\cdot}15$ respectively: ——, – – – –, · · · · ·, asymptotic theory; +, ×, ○, integral equation. (*a*) Magnitude $|f|$; (*b*) phase of $fe^{-ikx} = \delta_f$.

For family Q where $L = \Lambda$, the value of k ($\sim 6{\cdot}3$) is still smaller. Excellent agreement is found for f (figures 4*a*, *b*) and for transverse variations of ϕ at sections $\mathscr{A}$ and $\mathscr{B}$ (figure 5). In this family the largest kb is $\sim 0{\cdot}942$ ($0{\cdot}15 \times 2\pi$).

These generally remarkable agreements show that the asymptotic method is highly accurate even when $k = KL$ is only moderately large as long as $kb = KB$ is sufficiently small ($\leqslant 1{\cdot}2$).

A second factor affecting the accuracy of the asymptotic method is db/dx. For the same total length as P_3, we also computed a pencil-shaped raft with a blunt stern by two methods. While kb is also equal to $1{\cdot}885$, the forward section of the raft is much sharper than for P_3. It was found that the agreement over the forward part is much improved. Clearly, if $db(x)/dx$ is everywhere continuous, the agreement should no doubt be better.

To test the robustness of the asymptotic method still further, we examined a family of rectangular rafts R_i with $k = 4\pi$. The three different slenderness ratios are

$$B/L = 0{\cdot}05,\ 0{\cdot}1 \text{ and } 0{\cdot}14 \quad (R_1, R_2, R_3).$$

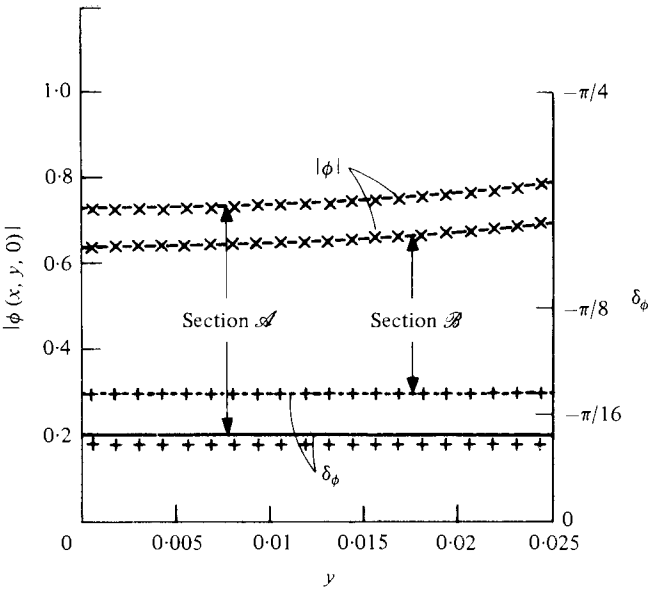

FIGURE 5. Normalized potential across the raft Q_1 with $L/\Lambda = 1$ and $B/L = 0{\cdot}05$. $\times$, $+$, asymptotic theory; ——, integral equation.

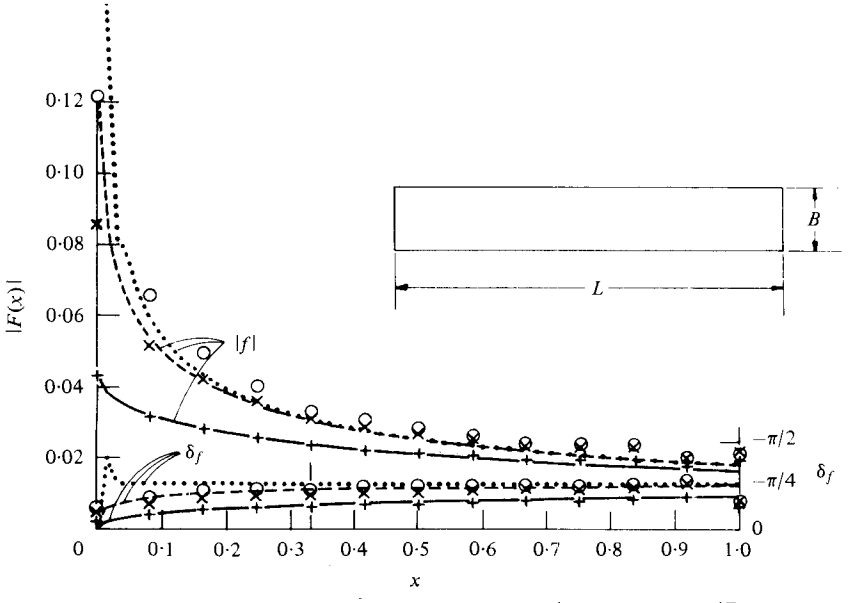

FIGURE 6. Normalized force along a rectangular raft with $L/\Lambda = 2$. For $B/L = 0{\cdot}05$, 0·10 and 0·15 respectively: ——, – – – –, · · · ·, asymptotic theory; $+$, $\times$, $\bigcirc$, integral equation.

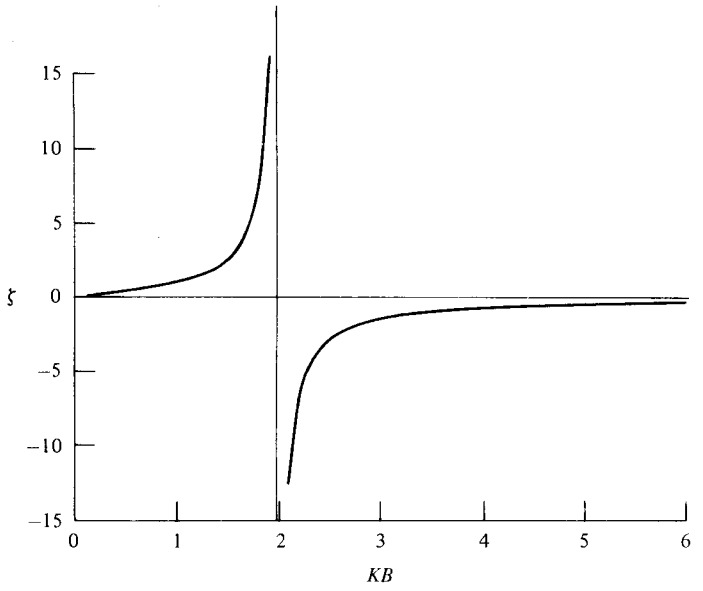

FIGURE 7. Singular behaviour of inner solution with ζ defined by (4.1).

Figure 6 shows the amplitude and argument of the force ($f(x)\exp(-ikx)$). The agreement between the two methods is excellent for the narrowest raft R_1, still very good for R_2, and discrepancies at the bow ($x = 0$) become quite evident for R_3.† This is quite natural since assumption (3.26) is clearly violated for blunt bows. Transverse variations of ϕ have been checked for R_1 at the section $x = 0$ (bow) and at the section $x = \frac{1}{3}$. Again discrepancy is very small towards the stern. It is also found that ϕ is essentially constant in y for small kb, suggesting a convenient approximation which eliminates the need to solve the transverse integral equation altogether. Plots are not presented here.

Finally, we report that the solution to the transverse integral equation becomes unbounded near $k_0 b = 1{\cdot}98615 \pm (4 \times 10^{-5})$. This is shown in figure 7 for the quantity

$$\zeta = \int_{-\frac{1}{2}kb}^{\frac{1}{2}kb} (1 + F'(u))du \tag{5.1}$$

as a function of kb. There is strong numerical evidence that the solution of (3.17) behaves as

$$F'(k, y) = \frac{F_0'(y)}{k - k_0} + O(1)$$

in the neighbourhood of $k_0 b$. This singularity affects the accuracy of (3.17) by a few per cent but still leads to a finite solution to the integral equation (3.34) whose right-hand side is zero for $k = k_0$. Furthermore, because $F''(x)$ is also zero at the singularity (see (3.32)), the inner solution is finite although the normalized inner solution $1 + F'(y)$ is not (see (3.35)). These conclusions have been numerically verified by studying a pencil-shaped raft with maximum $kb = 3$. The forces obtained by the asymptotic method compare well with the integral equation method at all values of kb including

† The case for $B/L = 0{\cdot}15$ has even greater discrepancy near the bow and is not presented.

the neighbourhood of $kb = 2$. In a note to be published, Yue & Mei (1981) give analytical and numerical evidence that the singularity is inherent in the boundary-value problem for F', is independent of the solution technique, and hence differs somewhat from the usual irregular frequency.

On the whole, the main advantage of the asymptotic method is that, within the limits of applicability, it is very economical in computation time and convenient for programming, in comparison with the integral equation method. Let the raft be discretized into N intervals longitudinally and no more than M intervals transversally. The computational time for the asymptotic theory is $O(NM^3)$ for solving N transverse integral equations, whereas the time for the two-dimensional integral equation method is $O(N^3M^3)$, if similar interpolating functions are used in both methods. Of course the latter method is not restricted to slender bodies or short waves.

We now turn our attention to an interesting application of the asymptotic method, namely wave energy extraction.

6. Application of the parabolic approximation to a wave-power absorber

An attractive way to extract energy from ocean waves has been invented by Masuda (1979) and is currently being tested in the Japan Sea. The device consists of a row of ten air turbines in as many vertical chambers opened along the keel of a ship. The ship is kept stationary in head seas by mooring lines and the waves resonate the water inside the chambers along the ship. These oscillating water columns create a variable pressure in the air trapped in the chambers, which in turn drives the turbines. A related device has also been suggested by French (1979), who uses flexible air bags floating on a slender frame. The breathing action of the bags as the waves pass by is used to produce high-pressure oil which in turn drives turbines.

It is possible to use the asymptotic method to study a device which crudely models the Masuda ship and, to some extent, the French bags. We consider a long slender body in head seas which absorbs wave power by controlling the pressure underneath its hull. To simplify the theory we idealize the ship as having zero draught (the ship may be supported on piles), and assume an infinite number of turbine chambers distributed uniformly over the entire keel. We also simplify the chamber–turbine system by a spring–mass-dashpot system (Evans 1978) which exerts on the water beneath a pressure equal to

$$P = (m\ddot{\xi} + c\dot{\xi} + \alpha\xi), \quad \text{where} \quad \xi = \eta(X, Y)e^{-i\omega T}, \tag{6.1}$$

where overhead dots denote time derivatives and m, c and α refer to unit area and are assumed to be constants. From kinematics we have

$$\dot{P} = m\dddot{\Phi}_Z + c\ddot{\Phi}_Z + \alpha\dot{\Phi}_Z. \tag{6.2}$$

Both equations are in physical variables.

Thus on the water surface directly interacting with the turbines

$$\ddot{\Phi} + g\Phi_Z = -\frac{\dot{P}}{\rho} = -\frac{1}{\rho}(m\ddot{\Phi}_Z + c\dot{\Phi}_Z + \alpha\Phi_Z). \tag{6.3}$$

Introducing the same dimensionless variables as in § 2, we get

$$\phi_z - k\phi = \beta\phi_z \quad \text{on} \quad z = 0, \tag{6.4}$$

where

$$\beta = \frac{1}{\rho g}(m\omega^2 - c) + \frac{i\alpha\omega}{\rho g}.$$

Defining

$$k' = k/(1-\beta), \tag{6.5}$$

which is in general complex, we have

$$\phi_z - k'\phi = 0 \quad \text{on} \quad z = 0. \tag{6.6}$$

In Masuda's ship the water column in the chamber is a part of the hydrodynamic system and the equivalent m and c may in general depend on ω. However, other resonant mechanisms without water columns are conceivable which may be closely approximated by constant m and c.

The same method of matched asymptotics may now be used. While the outer problem remains formally the same, the inner problem needs modification. The inner potential may be decomposed as in (3.1), (3.7) and (3.16), i.e.

$$\phi(x,y,z) = e^{ikx}\,\bar{\bar{F}}(x)\,[e^{kz} + \bar{F}(x,y,z)]. \tag{6.7}$$

The inner problem is governed by

$$\bar{F}_{yy} + \bar{F}_{zz} = k^2\bar{F}, \quad z < 0, \tag{6.8}$$

$$k\bar{F} - \bar{F}_z = 0, \quad z = 0 \quad \text{(domain } F\text{)}, \tag{6.9}$$

$$k'\bar{F} - \bar{F}_z = (k-k'), \quad z = 0 \quad \text{(domain } R\text{)}, \tag{6.10}$$

$$\bar{F} \to 0 \quad \text{as} \quad z \to -\infty, \tag{6.11}$$

$$\bar{F} \text{ does not grow exponentially as } k|y| \to \infty. \tag{6.12}$$

We use the Green function g defined in (3.18). It is easy to see that (3.14) still holds formally for $\bar{F}$ while the transverse integral equation becomes

$$\bar{F}(y) = (k-k')\int_{-\frac{1}{2}b(x)}^{\frac{1}{2}b(x)} g(y,0;y_0)\,(\bar{F}(y_0)+1)\,dy_0. \tag{6.13}$$

The numerical solution of (6.13) can be carried out in exactly the same way as for (3.15) or (3.17). The asymptotic value of the inner potential can also be derived:

$$\phi(x,y,z) \sim e^{ikx+kz}\,\bar{\bar{F}}(x)\left(1 + k(k-k')\,|y|\left[b(x) + 2\int_0^{\frac{1}{2}b(x)} \bar{F}(y_0)\,dy_0\right]\right), \quad k|y| \gg 1. \tag{6.14}$$

After matching with the outer solution the longitudinal integral equation is easily obtained:

$$1 - \frac{1+i}{2(\pi k)^{\frac{1}{2}}}\int_0^x \frac{\bar{V}(\xi)\,d\xi}{(x-\xi)^{\frac{1}{2}}} = \frac{\bar{V}(x)}{k(k-k')\left[b(x) + 2\int_0^{\frac{1}{2}b(x)} \bar{F}(y)\,dy\right]}. \tag{6.15}$$

This integral equation is solved exactly as (3.34). Once $\bar{V}$ is found, $\bar{\bar{F}}$ is given by

$$\bar{\bar{F}}(x) = \frac{\bar{V}(x)}{k(k-k')\left[b(x) + 2\int_0^{\frac{1}{2}b} \bar{F}(y)\,dy\right]} \tag{6.16}$$

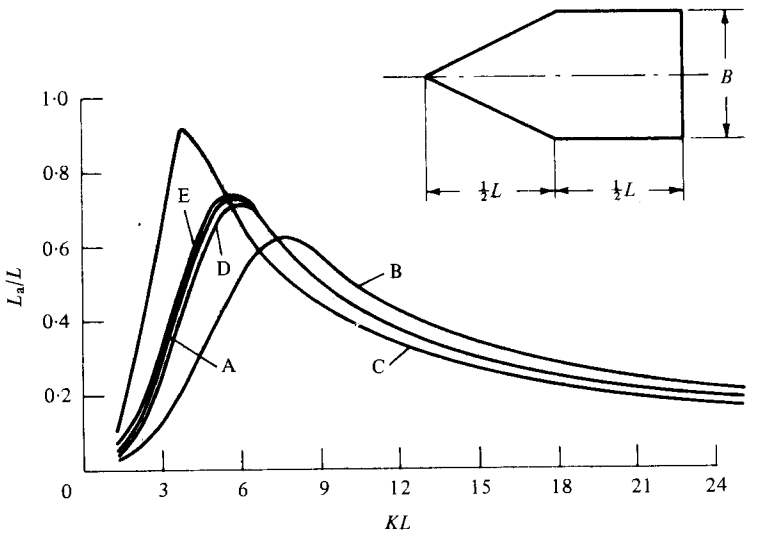

FIGURE 8. Variation of L_a/L *vs.* KL for ship S with $B/L = 0{\cdot}05$. Optimized at $KL = 2\pi$. A, $\beta = \beta_{\text{opt}}$; B, C, Re β = Re β_{opt} $(1 \pm 0{\cdot}1)$, $\alpha = \alpha_{\text{opt}}$; D, E, Re β = Re β_{opt}, $\alpha = \alpha_{\text{opt}}$ $(1 \pm 0{\cdot}2)$.

and the potential ϕ then follows from (6.7) and (3.14). The average power extracted is

$$P_w = \frac{\omega}{2\pi}\int_0^{2\pi/\omega} dT \int_0^L dX \int_{-\frac{1}{2}B(x)}^{\frac{1}{2}B(x)} \text{Re}\,(P)\,\text{Re}\,(\Phi_Z)\,dY \quad \text{on} \quad Z = 0. \tag{6.17}$$

We make use of (6.1), (6.4) and (2.7), and compute the time average to find

$$P_w = \frac{\rho g A^2}{2}\frac{g}{2\omega}\frac{2\Lambda}{\pi}(\text{Im}\,(\beta))\int_0^1 dx \int_0^{\frac{1}{2}b(x)} |\phi_z|^2\,dy, \quad z = 0. \tag{6.18}$$

Let us denote the incident wave power over a width L by

$$P_L = \frac{\rho g A^2}{2}\frac{g}{2\omega}L, \tag{6.19}$$

and further define L_a by

$$\frac{L_a}{L} = \frac{P_w}{P_L} = \frac{4}{k}(\text{Im}\,(\beta))\int_0^1 dx \int_0^{\frac{1}{2}b(x)} |\phi_z|^2\,dy. \tag{6.20}$$

Thus L_a is the absorption width, while L_a/L is the ratio of power extracted to power incident over a width equal to the raft length L, and is a measure of the efficiency of the device. An alternative form of L_a/L is

$$\frac{L_a}{L} = \frac{2\,\text{Im}\,(\beta)}{k^3}\left|\frac{k'}{k-k'}\right|^2 \int_0^1 \left|\frac{\bar{V}(x)}{b(x) + 2\int_0^{\frac{1}{2}b} \bar{F}(y)\,dy}\right|^2 \int_{-\frac{1}{2}b}^{\frac{1}{2}b} |1 + \bar{F}(y)|^2\,dy\,dx. \tag{6.21}$$

Attention will now be turned to the numerical results.

We study first the sample ship S depicted in the insert of figure 8, with slenderness ratio $B/L = b = 0{\cdot}05$. The extraction impedance $\beta = [(m\omega^2 - c) + i\alpha\omega]/\rho g$ which

$L/\Lambda = k/2\pi$	β_{opt}	L_a/L	L_a/Λ
0·7	$0{\cdot}81 \pm 0{\cdot}036i$	0·908	0·635
0·8	$0{\cdot}79 \pm 0{\cdot}038i$	0·836	0·669
0·9	$0{\cdot}76 \pm 0{\cdot}044i$	0·776	0·698
1·0	$0{\cdot}74 \pm 0{\cdot}046i$	0·727	0·727
1·2	$0{\cdot}69 \pm 0{\cdot}054i$	0·650	0·781
1·5	$0{\cdot}63 \pm 0{\cdot}061i$	0·569	0·854
2·0	$0{\cdot}54 \pm 0{\cdot}070i$	0·482	0·964
2·5	$0{\cdot}47 \pm 0{\cdot}074i$	0·426	1·069
3·0	$0{\cdot}41 \pm 0{\cdot}077i$	0·386	1·159
4·0	$0{\cdot}33 \pm 0{\cdot}076i$	0·334	1·338

TABLE 1. Optimum results for a range of k. $B/L = b = 0{\cdot}05$; shape of ship S in figure 8.

represents the behaviour of the 'turbines' T is chosen, by numerical tests, so as to maximize L_a/L at $k = 2\pi$, i.e. $L = \Lambda$. The optimum values for the system (S, T) are

$$L_a/L = 0{\cdot}727 \quad \text{for} \quad \beta_{\text{opt}} = 0{\cdot}74 + 0{\cdot}046i.$$

The variation of L_a/L with k for this sample ship is shown by curve A under the assumption that $\text{Re}\,\beta$ and the damping rate are kept fixed at the values which are optimal at $k = 2\pi$, i.e.

(i) $\text{Re}\,(\beta) = 0{\cdot}74 = \text{Re}\,(\beta_{\text{opt}})$,

(ii) $\text{Im}\,(\beta) = \left(\dfrac{\alpha_{\text{opt}}\omega_0}{\rho g}\right)\dfrac{\omega}{\omega_0} = 0{\cdot}046\,(\omega/\omega_0)$.

Condition (i) can be met by designing a turbine with $c = 0$ and m varying as $1/\omega^2$, or with $m = 0$ and c taking a constant negative value (both options may imply electronic control). The resulting efficiency curve shows a broad bandwidth since L_a/L is larger than 0·5 for $4 \leqslant k \leqslant 9$.

To understand better the influence of β on L_a/L we also test the sensitivity of the response curve to variations in $\text{Re}\,\beta$ and α_0. In figure 8 curves B, C, D and E correspond respectively to the following values:

$$\left.\begin{matrix}\text{B}\\ \text{C}\end{matrix}\right\} \quad \text{Re}\,\beta = (1 \mp 0{\cdot}1)\,\text{Re}\,\beta_{\text{opt}}, \quad \alpha = \alpha_{\text{opt}},$$

$$\left.\begin{matrix}\text{D}\\ \text{E}\end{matrix}\right\} \quad \text{Re}\,\beta = \text{Re}\,\beta_{\text{opt}}, \quad \alpha = (1 \mp 0{\cdot}2)\,\alpha_{\text{opt}}.$$

These efficiency curves appear to be rather independent of α but vary greatly with $\text{Re}\,\beta$. This can be explained crudely as follows: The efficiency is proportional to $[\bar{\eta}]^2$ where $[\bar{\eta}]^2$ is the averaged square amplitude of the displacement of the water surface under the ship. It is possible that, when the damping rate is decreased, $[\eta]^2$ increases in such a way that their product remains relatively constant. No such self-correcting effect exists for $\text{Re}\,\beta$ since its variation simply detunes the system, yielding a reduced efficiency. Quite naturally, an increase in the value of $\text{Re}\,\beta$ shifts the optimum frequency towards lower values and a decrease in $\text{Re}\,\beta$ shifts it towards higher values. Thus it is desirable to have an automatic control which can adjust $\text{Re}\,\beta$ according to the changing seas.

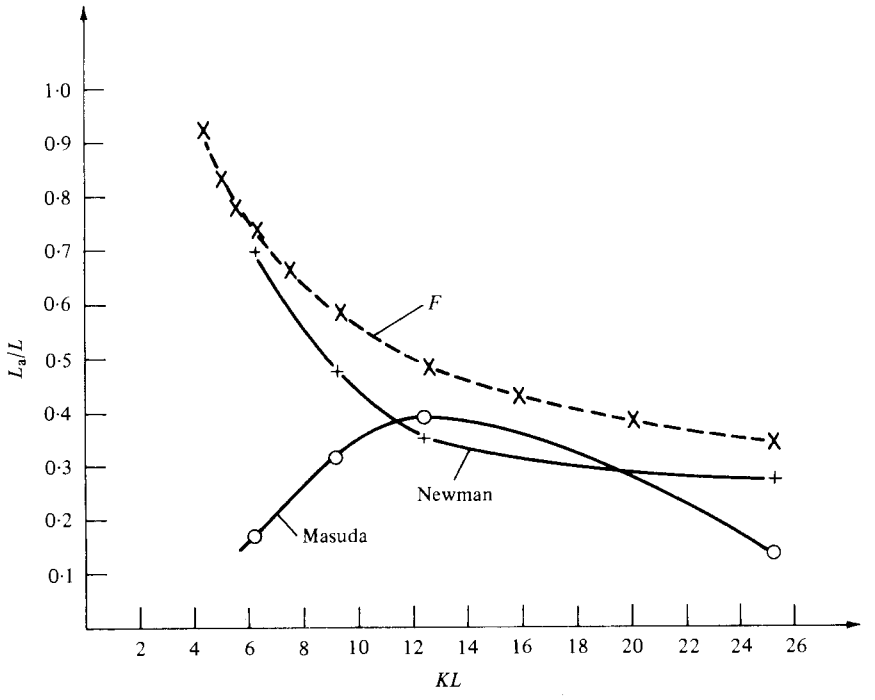

FIGURE 9. L_a/L *vs.* KL for ship S. Optimum for all KL according to present theory (F) as compared with Newman's theory and Masuda's experiments.

We then optimize L_a/L with respect to both real and imaginary parts of β for ten values of $k/2\pi = L/\Lambda$. The results are shown in table 1. Note that $\mathrm{Re}\,\beta$ is always positive, implying that the turbine–chamber system should have sufficient inertia or negative spring constant. The optimum efficiencies L_a/L are plotted as curve F in figure 9. For comparison we also show the estimate of Newman (1979) who did not inquire how optimization is achieved, and Masuda's experimental results.† Despite the differences in details between the actual Masuda ship and the theoretical model presented here, it is clear that much room is left for further optimization of Masuda's design.

By replotting the optimum efficiency curve F in figure 8 in terms of L_a/Λ, we have found (but do not show) that for the range of k considered L_a/Λ is approximated closely by the straight line $L_a/\Lambda \cong 0{\cdot}16\,(L/\Lambda) + 0{\cdot}6$. This result shows that for relatively small L/Λ the important reference scale to which L_a should be compared is the wavelength Λ but, for large values of L/Λ, L becomes the more appropriate reference scale and L_a approaches $0{\cdot}16L$ as the length of the ship goes to infinity.

Newman's results quoted in figure 9 are based on the assumption that the motion of the body consists of two orthogonal sinusoidal modes with argument kx. We have found (Haren 1980), however, that $|\eta|$ is non-uniform in x, being the greatest near midship and then steadily decreasing towards the stern. The phase of η, relative to the incident wave, increases almost linearly along the ship from a very small value at the bow to π at the stern. Clearly, our η corresponds to the sum of many trigonometric

† The results may have been influenced by the finite width of the wave tank.

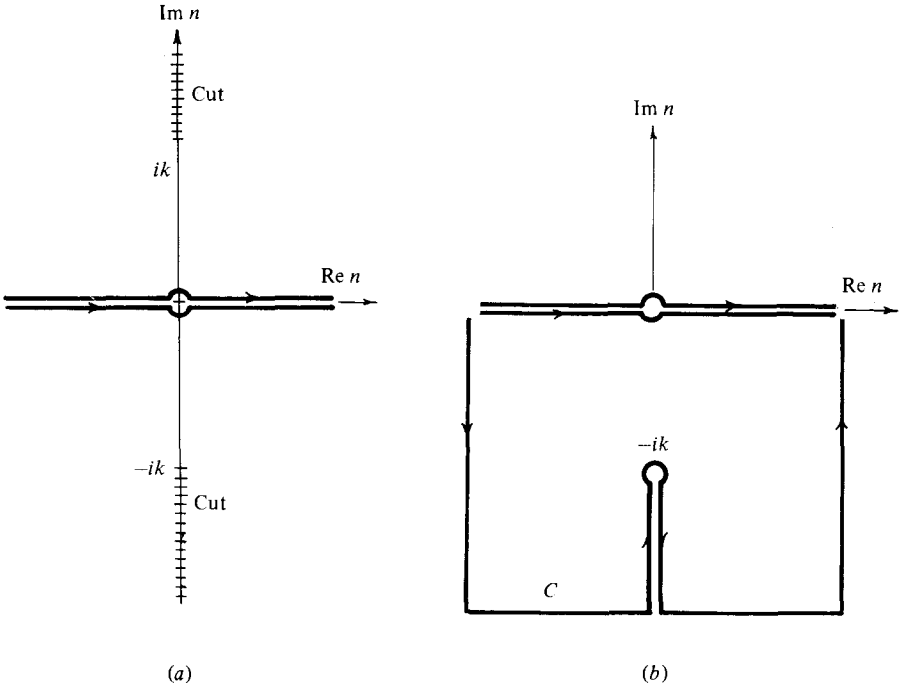

FIGURE 10. Contours of integration. (*a*) Original contours; (*b*) deformed contours.

modes and this larger degree of freedom explains why our efficiency in figure 9 is slightly better than Newman's. In principle still higher efficiency is possible if the turbine impedance is allowed to vary along the ship.

It should be remarked that the maximum magnitudes of $|\eta|$ under optimum conditions are 3, 4·2 and 7 for $b = 0{\cdot}5$, 0·1 and 0·05 respectively. The large amplitude for a very slender raft is undesirable both for violation of the linearized approximation and for the implied large stresses in the raft. One must then restrain the motion at the price of reduced efficiency (Newman 1979).

7. Concluding remarks

We have shown that, for head-sea incidence of short waves on a slender body, the parabolic approximation can be used for the intermediate far field, and leads quickly to the Abel integral equation after matching with the inner solution of Ursell. Within the stated limits, this asymptotic theory is simple, economical, and also accurate when compared with the integral equation method. The parabolic approximation has also been applied by Mei & Tuck (1980) to a ship moving at finite speed into head seas, in very shallow water (long wave theory) and appears to be equally feasible for deep water. However, it is as yet unclear whether extension to arbitrary incidence can be made.

We are grateful for the financial support of the U.S. Department of Energy (Contract DE-AC02-79-ET-21062) and the U.S. Office of Naval Research, Fluid Dynamics

Program (Contract NR062-228). We have profited from frequent discussions with Professors J. N. Newman, R. W. Yeung and F. Noblesse.

Appendix. Derivation of the Green function g for the inner problem

We look for $g(y,z;y_0)$ satisfying equations (3.10) to (3.13). Without any loss of generality we may take $y_0 = 0$ and write $g(y,z;0) = g(y,z)$. Since g is not growing exponentially, the solution can be found by Fourier transform in the sense of generalized functions (Lighthill 1967). The solution is easily found to be

$$g(y,z) = \frac{1}{2\pi}\frac{1}{2}\left\{\int_{-\infty}^{+\infty} + \int_{-\infty}^{+\infty}\right\}\frac{\exp\left(z(n^2+k^2)^{\frac{1}{2}}\right)e^{-iny}}{k-(n^2+k^2)^{\frac{1}{2}}}\,dn\Big\}, \tag{A 1}$$

where the contours are indented around the double pole at $n = 0$ as shown in figure 10(a). This choice of contour was first made by Ursell in order to render g symmetric in y.

For $(n^2+k^2)^{\frac{1}{2}}$ we choose the cuts along $[ik, i\infty]$ and $[-ik, -i\infty]$ and the branch so that $(n^2+k^2)^{\frac{1}{2}} \to |n|$ as $|n| \to \infty$ along the real axis.

Let us examine $y > 0$. The path of the two integrals are deformed to C as depicted in figure 10(b). After accounting for the residue,

$$g(y,z) = \frac{1}{4\pi}\left[-2\pi i\,\mathrm{Res}\,(0) + 2\int_C (-)\,dn\right]. \tag{A 2}$$

But the integral in (A 2) has contributions only along the two sides of the branch cut because y is positive and $\exp z(n^2+k^2)^{\frac{1}{2}}/(k-(n^2+k^2)^{\frac{1}{2}})$ vanishes uniformly as $|n| \to \infty$. Along the two sides of the branch cut

$$(n^2+k^2)^{\frac{1}{2}} = \pm i(|n|^2-k^2)^{\frac{1}{2}} \quad \text{on the } \begin{Bmatrix}\text{left-hand}\\ \text{right-hand}\end{Bmatrix} \text{side}.$$

Hence the integral in (A 2) may be written as

$$\begin{aligned}\int_C (\,)\,dn &= i\int_k^\infty e^{-vy}\,dv\left(\frac{\exp\left[iz(v^2-k^2)^{\frac{1}{2}}\right]}{k-i(v^2-k^2)^{\frac{1}{2}}} - \frac{\exp\left[-iz(v^2-k^2)^{\frac{1}{2}}\right]}{k+i(v^2-k^2)^{\frac{1}{2}}}\right)\\ &= -2\int_k^\infty \frac{e^{-vy}}{v^2}\left[k\sin\left(z(v^2-k^2)^{\frac{1}{2}}\right) + (v^2-k^2)^{\frac{1}{2}}\cos\left(z(v^2-k^2)^{\frac{1}{2}}\right)\right]dv. \end{aligned} \tag{A 3}$$

The residue at $n = 0$ is

$$\mathrm{Res}\,(0) = \lim_{n\to 0}\frac{d}{dn}\left(\frac{n^2\exp\left[z(n^2+k^2)^{\frac{1}{2}} - iny\right]}{k-(n^2+k^2)^{\frac{1}{2}}}\right) = 2iky e^{kz}. \tag{A 4}$$

Using the symmetry of g with respect to y, we finally get

$$g(y,z) = k|y|e^{kz} - \frac{1}{\pi}\int_k^\infty \frac{e^{-v|y|}}{v^2}\left(k\sin\left(z(v^2-k^2)^{\frac{1}{2}}\right) + (v^2-k^2)^{\frac{1}{2}}\cos\left(z(v^2-k^2)^{\frac{1}{2}}\right)\right)dv. \tag{A 5}$$

If the source point is at y_0, we should replace $|y|$ by $|y-y_0|$ in (A 5). On the body ($z = 0$) the expression is much simpler:

$$g(y,0) = k|y| - \frac{1}{\pi}\int_k^\infty \frac{e^{-v|y|}}{v^2}(v^2-k^2)^{\frac{1}{2}}\,dv. \tag{A 6}$$

The integral above can be evaluated in a more convenient way with the successive changes of variables $v = kt$ and $t = \cosh u$. The final expression for $g(y, 0)$ is then

$$g(y,0) = k|y| - \frac{1}{\pi} K_0(k|y|) + \frac{1}{\pi}\int_0^\infty \frac{\exp(-k|y|\cosh u)}{\cosh^2 u}\, du. \tag{A 7}$$

The integral in (A 7) is very easy to evaluate numerically. An accuracy within 10^{-6} can be achieved by taking the upper limit to be 8 for $k|y| = 0$. The range of integration can be further reduced for increasing $k|y|$.

It is also possible to obtain an asymptotic expansion of $g(y, 0)$ for large $k|y|$. From equation (A 5) it is easy to see that $(g(y,z) - e^{kz} k|y|)$ decays exponentially for $k|y| \gg 1$:

$$\begin{aligned} |g(y,z) - k|y| e^{kz}| &\leqslant \left|\frac{k}{\pi}\int_k^\infty \frac{e^{-v|y|}}{v^2} dv\right| + \left|\frac{k}{\pi}\int_k^\infty \frac{e^{-v|y|}}{v} dv\right| \\ &\leqslant \frac{e^{-k|y|}}{\pi}\left(1 + \int_k^\infty \frac{e^{-(v-k)|k|}}{v}\right) \\ &\leqslant \frac{e^{-k|y|}}{\pi}(1 + 1/k|y|). \end{aligned}$$

Hence the asymptotic expansion is

$$g(y,z) = k|y| e^{kz} + O(e^{-k|y|}) \quad \text{for} \quad k|y| \gg 1, \tag{A 8}$$

which behaves as the submerged source of Ursell (1968).

REFERENCES

Bai, K. J. & Yeung, R. 1974 Numerical solutions of free surface flow problems. *Proc. 10th Symp. Naval Hydrodynamics, Cambridge, MA*, pp. 609–647.

Chen, H. S. & Mei, C. C. 1974 Oscillations and wave forces in a man-made harbor in the open sea, *Proc. 10th Symp. Naval Hydrodynamics, Cambridge, MA*, pp. 573–596.

Evans, D. V. 1978 The oscillations water column wave-energy device. *J. Inst. Maths. Applics.* **22**, 423–433.

Faltinsen, D. M. 1971 Wave forces on a restrained ship in head-sea waves. Ph.D. thesis, Naval Architecture Dept., University of Michigan.

Faltinsen, D. M. 1972 Wave forces on a restrained ship in head-sea waves. *Proc. 9th Symp. Naval Hydrodynamics, Paris, France*, pp. 1763–1840.

French, M. J. 1979 The search for low cost wave energy and the flexible bag device. *Symp. on Ocean Wave Energy Utilization, Gothenburg, Sweden*, pp. 364–377.

Garrison, C. J. 1969 On the interaction of an infinite shallow draft cylinder oscillating at the free surface with a train of oblique waves. *J. Fluid Mech.* **39**, 227–255.

Haren, P. 1980 Wave energy: a hydrodynamic analysis of head-sea absorbers. Ph.D. thesis, Dept. of Civil Engineering, Massachusetts Institute of Technology.

Haskind, M. D. 1954 On wave motions of a heavy fluid. *Prikl. Mat. Mekh.* **18**, 15–26. (In Russian.)

Kim, W. D. 1963 On the forced oscillations of shallow-draft ships. *J. Ship Res.* **7**, 7–18.

Liapis, N. & Faltinsen, O. M. 1980 Difffraction of waves around a ship. *J. Ship Res.* **24**, 147–155.

Lighthill, M. J. 1967 On waves generated in dispersive systems by travelling forcing effects, with applications to the dynamics of rotating fluids. *J. Fluid Mech.* **27**, 725–752.

Maruo, H. & Sasaki, N. 1974 On the wave pressure acting on the surface of an elongated body fixed in head sea. *J. Soc. Naval Arch. Japan* **136**, 34–42.

MASUDA, Y. 1979 Experimental full scale result of wave power machine Kaimei in 1978. *Symp. on Wave Energy Utilization, Gothenburg, Sweden*, pp. 349–363.

MEI, C. C. 1979 Grazing incidence of short elastic waves on a slender cavity. In *Wave Motion*, vol. 1, pp. 113–122.

MEI, C. C. & TUCK, E. O. 1980 Forward scattering by long thin bodies. *SIAM J. Appl. Math.* (to appear).

NEWMAN, J. N. 1979 Absorption of wave energy by elongated bodies. *Appl. Ocean Res.* **1**, 189–196.

SKJØRDAL, S. O. & FALTINSEN, O. M. 1980 A linear theory of springing. *J. Ship. Res.* (to appear).

URSELL, F. 1968 On head seas travelling along a horizontal cylinder. *J. Inst. Maths Applics.* **4**, 414–427.

URSELL, F. 1977 The refraction of head seas by a long ship. Part 2. Waves of long wavelength. *J. Fluid Mech.* **82**, 643–657.

WEHAUSEN, J. V. & LAITONE, E. V. 1960 Surface waves. *Handbuch der Physik*, vol. IX, pp. 446–778. Springer.

YEUNG, R. W. 1973 A singularity distribution method for free-surface flow problems with an oscillating body. *College Engng, Univ. of Calif., Berkeley, Rep.* NA 73–6.

YUE, D. K. P., CHEN, H. S. & MEI, C. C. 1978 A hybrid element method for diffraction of water waves by three-dimensional bodies. *Int. J. Num. Methods in Engng* **12**, 245–266.

YUE, D. K. P. & MEI, C. C. 1981 Note on the singularity of an inner problem for head-sea diffraction by a slender body. *J. Fluid Mech.* (to appear).